Received July 6, 2020, accepted July 13, 2020, date of publication July 17, 2020, date of current version August 7, 2020.

Digital Object Identifier 10.1109/ACCESS.2020.3010026

Research on a Novel GaN-Based Converted Mini-LED Backlight Module via a Spectrum-Decouple System

CHE-HSUAN HUANG[1], SHU HSIU CHANG[2], BEEN-YU LIAW[3], CHENG-YI LIU[4], CHIA-YUEH CHOU[4], JIA-ROU ZHOU[5], CHIEN-CHUNG LIN[2], (Senior Member, IEEE), HAO-CHUNG KUO[5], (Fellow, IEEE), LI-JUN SONG[6], FENG LI[1], AND XINKE LIU[1], (Member, IEEE)

[1]Guangdong Research Center for Interfacial Engineering of Functional Materials, College of Materials Science, College of Electronics and Information Engineering, Shenzhen University, Shenzhen 518060, China
[2]Institute of Photonic System, National Chiao Tung University, Hsinchu City 30010, Taiwan
[3]College of Information Science and Engineering, Fujian University of Technology, Fuzhou 350108, China
[4]Department of Chemical and Materials Engineering, National Central University, Taoyuan City 32001, Taiwan
[5]Department of Photonics, Institute of Electro-Optical Engineering, National Chiao Tung University, Hsinchu City 30010, Taiwan
[6]Research Center of Guangdong Intelligent Charging and System Integration Engineering Technology, Shenzhen Winsemi Microelectronics Company Ltd., Shenzhen 518000, China

Corresponding author: Xinke Liu (xkliu@szu.edu.cn)

This work was supported by National Key Research and Development Program of China (2017YFB0403000 and 2017YFB0404100), National Natural Science Foundation of China (61974144), Key-Area Research and Development Program of Guangdong Province (2020B010169001), and the National Taipei University of Technology-Shenzhen University Joint Research Program (2020009).

ABSTRACT Owing to the development of modern display technology, micro- and mini-light-emitting diodes (LEDs) have affected technological advancements in the display industry. The structure of mini-LEDs is completely different than that of traditional LED backlights because the former employs a display technology with an LED array structure, optical resonant cavity, and color conversion layer. Display backlight technology encounters difficulty in achieving a truly effective energy-loss mechanism when designing or measuring mini-LED performance. The present study proposes three major mini-LED energy loss mechanisms: cross-talk, resonant, and quantum conversion losses. Herein, the spectrum was obtained through the integrating sphere system, and the calculation mechanism was formed by the down-conversion theorem as the decoupling principle, which successfully calculated the independent energy-loss efficiency of each mechanism and effectively deduced the brightness and color saturation performance of this design combination.

INDEX TERMS Mini-light-emitting diode, energy loss, display, backlight, down-conversion theorem.

I. INTRODUCTION

In recent years, backlight technologies for display industry have reached maturity because of light-emitting diodes (LEDs), which have unique characteristics, such as long lifetime [1], high efficiency, and energy-saving properties [2]. Among the new generation of display technologies, micro-LEDs are the most popular and are highly anticipated in the market [3]. Micro-LED display technology has the advantages of high dynamic contrast [4] and high color saturation [5], and it has become a widely discussed display solution with high potential. However, as the life attenuation of gallium nitride (GaN)-based and gallium arsenic (GaAs)-based LEDs is inconsistent, production of mini-LEDs that use the same GaN-based light source array to excite color conversion diaphragms has become part of mainstream technology.

The architecture of a mini-LED backlight includes (1) a blue light array and (2) a color conversion diaphragm [6]. Owing to the differences in the design of single light sources, blue light arrays with different shape designs have various light extraction efficiencies, including angle light extraction characteristics and freeform-designed chip-scale package [7]

The associate editor coordinating the review of this manuscript and approving it for publication was Wei Wang.

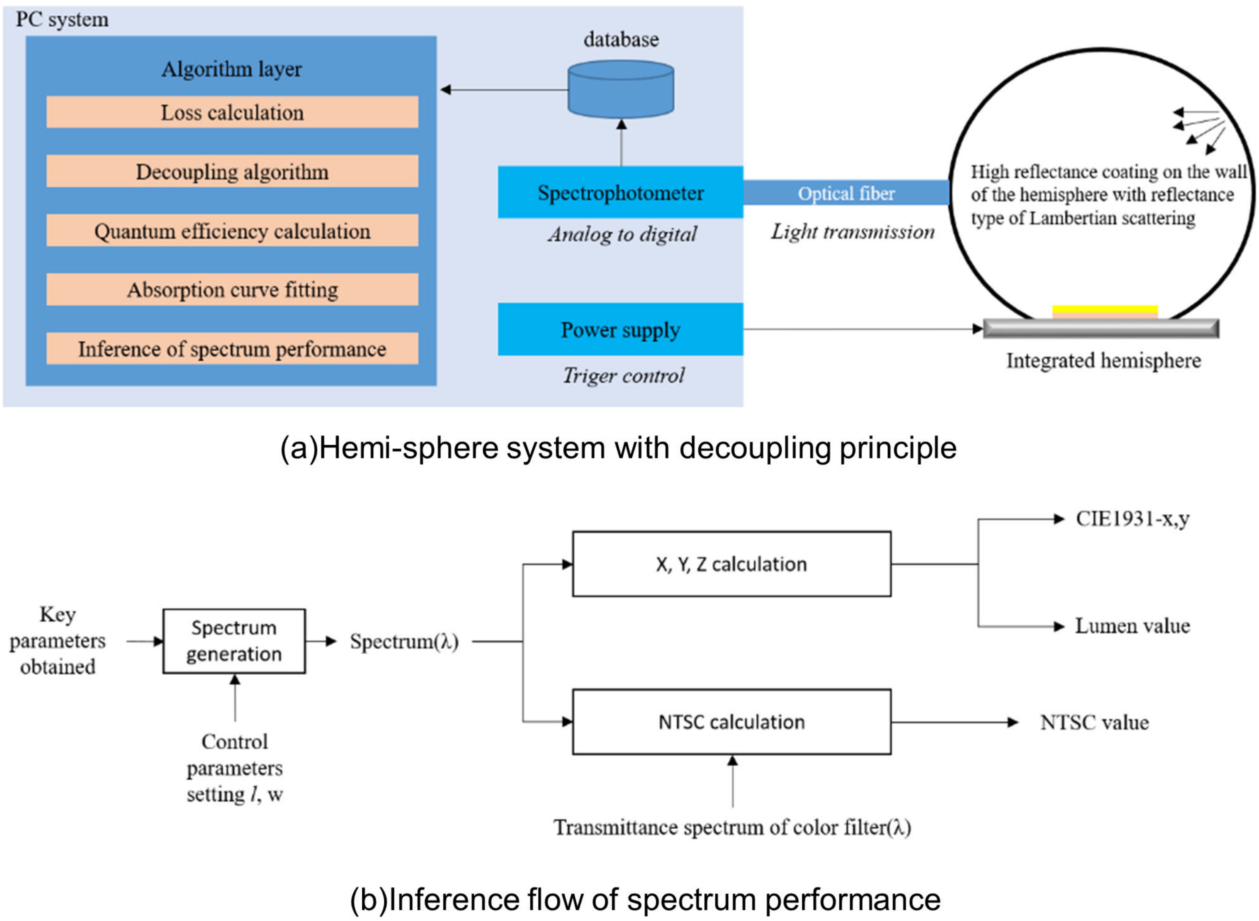

FIGURE 1. **(a) Hemisphere system with decoupling principle, (b) Inference flow of spectrum performance.**

with large luminous angle characteristics that have significant advantages. In the light color conversion technology, due to the evolution of phosphor and quantum dots in packaging technology [8]–[10], stable high color saturation requirements have been achieved. As the manufacturing technology matures, the design and measurement of mini-LEDs are expected to gradually become important. At present, with the maturity of mini-LEDs, many studies have been conducted on image quality; however, in comparison to energy loss studies, technology has not matured enough for the testing of measurement methods.

As the current mini-LED design is mainly based on energy transfer, color performance, and other important indicators, no suitable method for design and analysis is currently available. Thus, this study proposes a design process by referring to the work of Schlotter *et al.* on the mechanism of blue-pumped white LED [11]. We have successfully derived the calculation process that can be successfully implemented. Through this study, three energy-loss modes of mini-LED can be analyzed: (1) cross-talk, (2) resonant, (3) and down-conversion losses. The down-conversion loss of multiple excitation sources is always difficult to effectively verify and predict due to complex color conversion and optical path problems [12]. Therefore, herein we propose the following conversion theory as the core of down-conversion loss. Through six configuration experiments, the proposed measurement method determines that the loss mechanism of light energy and the conversion efficiency can be quantified in a mini-LED system.

II. PRINCIPLE AND THEORY

A. INTRODUCTION TO MEASUREMENT SYSTEM

Since mini-LEDs are designed using multiple chip arrays, they have tighter pitch than the traditional backlight solution. Mini-LED solutions experience significant loss between the chip array and the space between the light source and quantum conversion layer. To optimize the design of mini-LEDs, the measurement system architecture used in this study is shown in Fig. 1(a), which includes the following: (1) high reflection and high scattering barium sulfate-coated integrating sphere, (2) collection of optical fiber and power supply, (3) spectroscopic spectrometer, (4) personal computer system, (5) loss calculation, (6) decoupling algorithm, (7) quantum efficiency calculation, (8) absorption curve fitting, and (9) inference of spectrum performance. This architecture aims to minimize the gaps when material parameters are

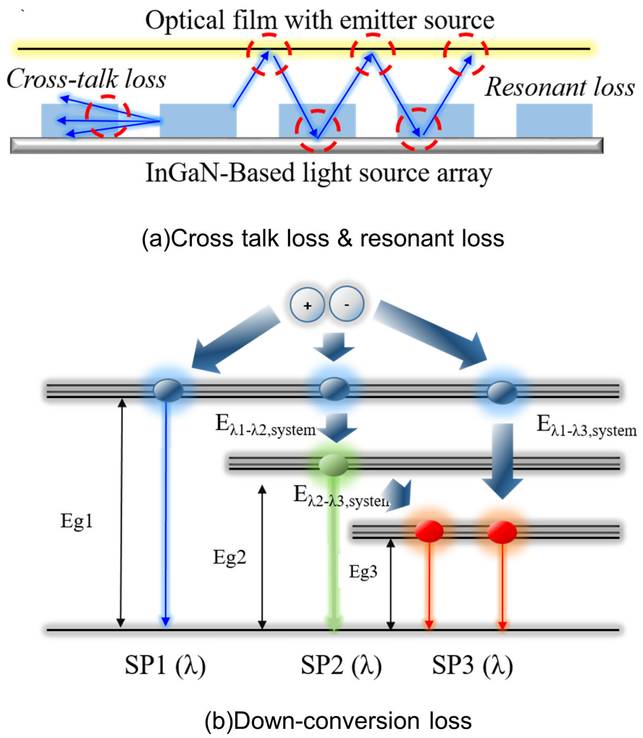

FIGURE 2. **Schematic of (a) cross-talk loss and resonant loss, (b) down-conversion loss.**

individually measured and are measured in an actual environmental system. The actual sample is used as the parameter to obtain the source. The energy error caused by the neglect of the large-angle light in the common image measurement system is reduced through the integrating sphere structure. The sample of mini-LEDs array used in this study comprises a GaN-based chip with a size of 5 mil × 9 mil and a 2 mm pitch between the nearest neighbor chips.

After the spectrum is obtained and calculations are conducted, this system can collect each key energy conversion efficiency parameters and convert them into a spectrum prediction model to fine-tune the parameters, and then, the system can calculate it as lumen after the process calculation [13], as shown in Fig. 1(b) vs Commission international declaring (CIE)-x and CIE-y and national television system committee (NTSC) vs CIE-x and CIE-y results; these results are modeled through the actual measurement data. This mechanism can effectively eliminate the environmental difference between the material parameter measurement and actual sample measurement to achieve a high degree of simulation model construction and performance prediction.

B. THREE MAIN LOSS MECHANISMS

As shown in Fig. 2, the mini-LED backlight unit (BLU) architecture involves three major loss mechanisms: (1) cross talk, (2) resonant, and (3) quantum conversion losses.

As shown in Fig. 2(a), from the perspective of beam tracing, as the GaN-based LED has multi-faceted light-emitting characteristics, the aspect ratio of its size can affect the proportion of light emitted from each face. Thus, when an LED array is formed, part of the light emitted by each chip will be absorbed by the surrounding chips and cause losses. Owing to this loss, the overall mini-LED array spacing, substrate materials, and volumes of each surface of the wafer have subtle structural differences [14]–[16]. Every small difference will affect the overall loss. The effect is difficult to measure solely based on the amount of material parameters. Furthermore, since a resonant cavity forms between the LED array and optical conversion diaphragm when the light travels to the edge of the optical diaphragm, reflection and refraction occur, and the reflected light changes based on the difference of the materials. The diffuse reflection angle and reflectivity at this boundary cause loss of light energy. The light reflected back to the LED array at this boundary is absorbed and reflected by the LED and substrate materials. Repetition of the above mechanism causes a resonant loss in the overall structure. Similarly, due to the excessive unpredictability and elasticity of the surface reflection and absorption characteristics of each material, the traditional material parameter measurement adopts the beam tracing method, and thus, immersive simulation of the effect cannot be achieved.

In addition, the light passing through the boundary of the optical film enters the light conversion layer in the film. This conversion layer is typically formed by particles with high down-conversion efficiency. A good backlight source usually comprises two or more wavelengths. As shown in Fig. 2(b), the conversion layer with two conversion particles have three light conversion processes during the down-conversion process: (1) λ1 is defined as the emission wavelength of the excitation light source; λ2 and λ3 are the emission wavelengths of the stimulated emission light source of shorter wavelength and longer wavelength, respectively. (2) The light energy that has not been absorbed or converted by the light conversion layer forms the λ1 emission wavelength in the system. (3) White light is formed in the system. The λ2 emission wavelength originates from the photon energy after being absorbed in the light conversion layer and is down-converted, excluding the energy absorbed by the λ3 emitter. In this process, Stoke's shift loss, quantum efficiency, and the system or λ3 emitter absorbed energy loss are involved. (4) The origin of the λ3 emission wavelength in the system is the absorption of λ1 and λ2 light and the emission of the down conversion. Stoke's shift loss, quantum efficiency, and the energy loss absorbed by the system are also involved in this mechanism.

The aforementioned three major energy-loss processes are the main energy-loss mechanisms in the mini-LED BLU module.

C. ALGORITHM DERIVATION I: SINGULAR EMITTER MODEL FORMS DOWN-CONVERSION LUMINOUS EFFICIENCY THEORY

Down-conversion luminous efficiency (DCLE) [17] is applied to study the optic model of white light LED. The total output power (P_{LED}) of the white light out of a single emitter comprises (1) residual (leaked) pumping light and

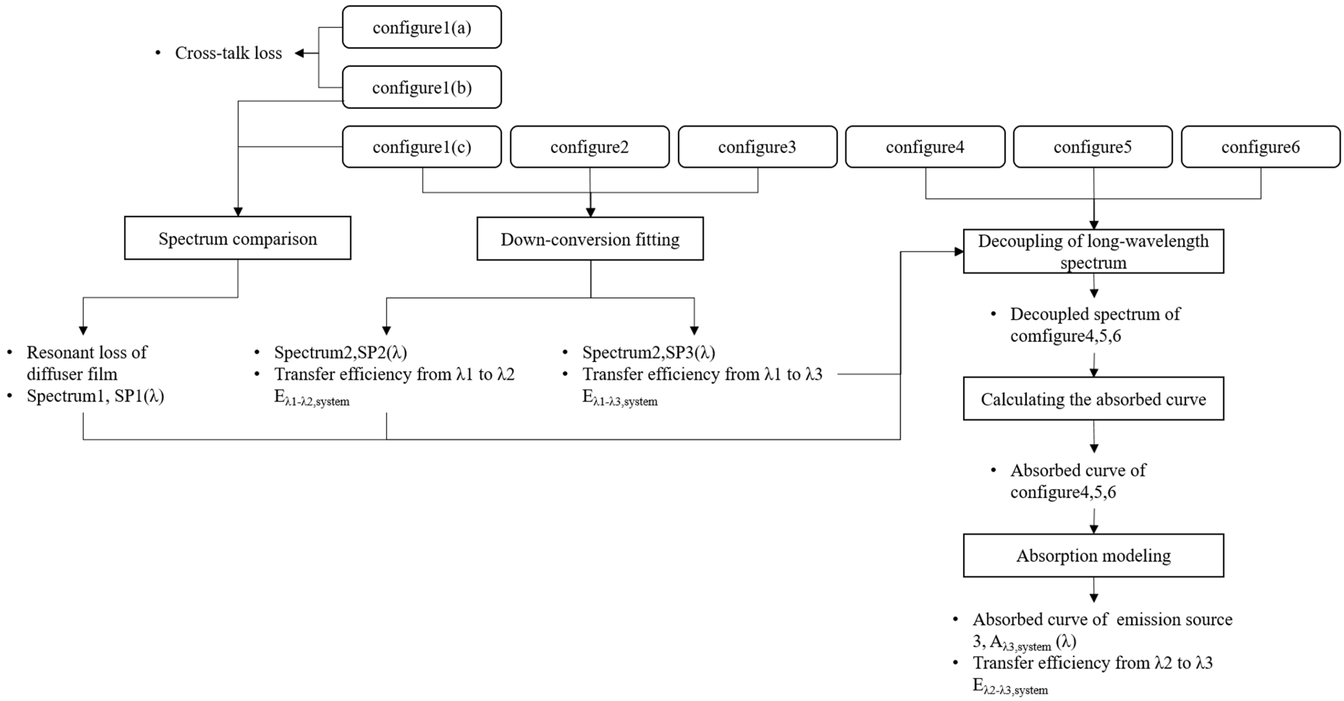

FIGURE 3. Flow chart of parameter acquisition.

(2) down-converted light, which are expressed as follows:

$$l \cdot P_{\mathrm{LED}} \cdot POE_b \tag{1}$$

$$(1-l) \cdot P_{LED} \cdot \mathrm{QE}_{ph} \cdot S_{\lambda p-\lambda ph} \cdot POE_p \tag{2}$$

where l is the fraction of the pumping light leakage, QE_{ph} is the quantum efficiency of the emitter, $S_{\lambda p-\lambda ph}$ is the Stoke's shift of the material, and POE_b and POE_p are the optical extraction efficiencies for pumping and emission sources (similar to emitters), respectively.

Down-conversion theorem clearly explains the generation of white light. However, accurately measuring all the parameters in the aforementioned two equations is difficult. To establish a precise model of the white-light LED, the pumping light, as shown in equation (1), is simplified as follows:

$$l \cdot P_{B-LED,} \tag{3}$$

where P_{B-LED} is the radiant flux of the blue LED array. Moreover, P_{B-LED} equals to $P_{LED} \cdot POE_b$, which can be directly measured from the blue GaN-based LED array. On the other hand, the down-converted light can be written as

$$(1-l) \cdot P_{B-LED} \cdot \left(\frac{POE_p}{POE_b}\right) \cdot E_{\lambda p-\lambda ph1} \tag{4}$$

where the $P_{LED} \cdot POE_p$ and $QE_{ph} \cdot S_{\lambda p-\lambda ph}$ in equation (2) are replaced by $P_{B-LED} \cdot (POE_p/POE_b)$ and $E_{\lambda p-\lambda ph1}$, respectively. The parameter $E_{\lambda p-\lambda ph1}$ depicts the efficiency of the material, as light is emitted by the pumping source in the system. In equation (4), $\mathrm{P_{LED}}$ can be measured, but POE_b, POE_p, and $\mathrm{E}_{\lambda p-\lambda ph1}$ are still difficult to measure. Although some parameters are unavailable, we can still create a precise LED model by combining the items that are indirectly obtained. Thus, the equation (4) can be written as follows:

$$(1-l) \cdot P_{B-LED} \cdot E_{\lambda 1-\lambda 2,\mathrm{system}} \tag{5}$$

where $\mathrm{E}_{\lambda 1-\lambda 2,\mathrm{system}}$ is the parameter that involves the light extraction efficiency of the blue light, the emission light, and material's original quantum efficiency. Furthermore, the parameter ($\mathrm{E}_{\lambda 1-\lambda 2,\mathrm{system}}$) can be calculated using equation (5) with l equal to 0 and equation (3) with l equal to any value. The singular scatter system had been successfully proven in a previous study [18].

D. ALGORITHM DERIVATION II: DUAL-EMITTER MODEL BASED ON DOWN-CONVERSION LUMINOUS EFFICIENCY THEORY

According to the preceding discussions, the singular emitter model can precisely describe the energy transfer of the pumping and emission lights. However, the singular emitter model is insufficient for describing the energy transfer of the dual emitter model. To refine the model of the dual emitter, we have to consider the energy transfer between emitters.

The dual emitter model is based on the hypothesis that a slight up-conversion energy transfer occurs. Only the down-conversion energy transfer exists in the model [19]. Thus, the energy transfer of the dual emitter is calculated by the sequence of the emission spectrum wavelength. First, the singular emitter model is calculated as equation (6), and the spectrum of the singular emitter LED, LED(λ), can be presented as follows:

$$\mathrm{LED}(\lambda) = l \cdot P_{\mathrm{B-LED}} \cdot SP1(\lambda) + (1-l) \cdot P_{\mathrm{B-LED}} \cdot E_{\lambda 1-\lambda 2,\,\mathrm{system}} \cdot SP2(\lambda), \quad (6)$$

where SP1(λ) is the normalized emission spectrum of the pumping source and SP2(λ) is the normalized spectrum of the emitter with a shorter wavelength.

The dual emitter model is considered based on the emitter with a longer wavelength added to the singular system that has a spectrum LED (λ). According to the stimulated absorption, the emitter with a longer wavelength can better absorb the energy of the shorter wavelength than that of the longer wavelength. Equation (7) presents the energy, which is absorbed. The A(λ) in equation (7) is the absorption curve of the emitter with a longer wavelength emission:

$$AE = \int_{780}^{380} \mathrm{A}(\lambda)\,\mathrm{LED}(\lambda)\,d\lambda. \quad (7)$$

Equation (7) can be written as equations (8) and (9). These equations indicate two parts of absorbed items in the dual-emitter LED system. The first part is contributed by the pumping source, $\mathrm{AE}_{\lambda 1}$, and the second, $\mathrm{AE}_{\lambda 2}$, is contributed by the energy emitted from the emitter with a shorter emission wavelength.

$$\mathrm{AE} = \int_{380}^{780} \mathrm{A}(\lambda) \cdot [l \cdot P_{\mathrm{B-LED}} \cdot \mathrm{SP1}(\lambda) + (1-l) \cdot P_{\mathrm{B-LED}} \cdot E_{\lambda 1-\lambda 2,\,\mathrm{system}} \cdot SP2(\lambda)]\,d\lambda, \quad (8)$$

$$\mathrm{AE} = \mathrm{AE}_{\lambda 1} + \mathrm{AE}_{\lambda 2} \quad (9)$$

After the absorption process, the spectrum of the singular emitter system can be presented as follows:

$$\mathrm{LED}'(\lambda) = [\,l \cdot P_{\mathrm{B-LED}} \cdot SP1(\lambda) + (1-l) \cdot P_{\mathrm{B-LED}} \cdot E_{\lambda 1-\lambda 2,\,\mathrm{system}} \cdot SP2(\lambda)] \cdot \left(1 - \mathrm{A}_{\mathrm{system}}(\lambda)\right), \quad (10)$$

where $\mathrm{A}_{\mathrm{system}}(\lambda)$ is the absorption from the total system of the mini-LED backlight.

Then, the wavelength of the absorbed photons is converted to the emission wavelength through the conversion efficiency, $\mathrm{E}_{\lambda 1-\lambda 2,\mathrm{system}}$ and $\mathrm{E}_{\lambda 2-\lambda 3,\mathrm{system}}$. It also includes the loss by Stoke's shift and quantum efficiency. After these processes, the spectrum of the dual-emitter system can be presented as follows:

$$\mathrm{LED}''(\lambda) = \mathrm{LED}'(\lambda) + \left[\mathrm{AE}_{\lambda 1} \cdot E_{\lambda 1-\lambda 3,system} + \mathrm{AE}_{\lambda 2} \cdot E_{\lambda 2-\lambda 3,system}\right] \cdot SP3(\lambda) \cdot \left(1 - \mathrm{A}_{\mathrm{system}}(\lambda)\right) \quad (11)$$

where SP3(λ) is the normalized spectrum of emitters with longer wavelengths.

After obtaining the parameters in the equation, this study aims to predict the brightness and color performance by modulating the fraction of the pumping light leakage and the absorption coefficient for the designer's reference.

III. EXPERIMENT FLOW

Algorithm derivation is described below. Similar to the singular emitter system, the parameters are difficult to precisely measure. To enhance the accuracy of the dual emitter model, we design a method called experiment-algorithm hybrid method. Fig. 3 shows the parameter accessing progress of the hybrid method in the dual emitter system.

Initially, we prepared six configurations with different amounts of emitters in the optical system. These configurations are shown in Table 1.

To acquire necessary parameters, a process is designed to obtain the key parameters of the dual emitter model. As shown in Fig. 4, this set of method includes six well-designated configurations and two types of algorithms for decoupling and fitting. By measuring the parameters and performing the experiments on the same platform, the inaccuracy/discrepancy between the two systems can be reduced.

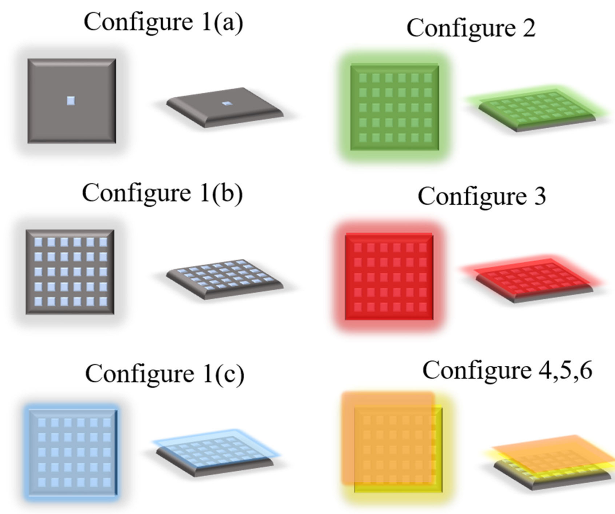

FIGURE 4. Schematic of experiment configuration.

In this method, the radiant flux and emission spectrum of the pumping source was directly obtained from configuration 1. Then, based on the comparison of the spectra of configurations 1, 2, and 3, the items of the absorbed and emitted energy by emission sources 1 and 2 can be calculated. Thereafter, the block "fitting by DCLE theorem" indicates the method for calculating the efficiencies of the emission sources 1 and 2. The spectra of the emission sources 1 and 2 are also obtained through the process of "fitting by DCLE theorem," as described in the equations in the above section. Configurations 4, 5, and 6 are types of the dual emitter mixing systems. The spectra of these three configurations are affected by the absorption of emission source 2, which is usually the most difficult parameter to procure in this method. The block "decoupling the mixing spectrum" presents the principle to decouple the mixing spectrum. The principle has to be maintained where the spectrum shape of the emission source with a longer emission wavelength is unchanged. This condition implies that the range of the longer wavelength

TABLE 1. Target parameters.

	Configuration 1	Configuration 2	Configuration 3	Configuration 4	Configuration 5	Configuration 6
Spectrum composition	Spectrum 1 (Pumping spectrum)	Spectrum 1 + Spectrum 2	Spectrum 1 + Spectrum 3	Spectrum 1 + Spectrum 2 + Spectrum 3	Spectrum 1 + Spectrum 2 + Spectrum 3	Spectrum 1 + Spectrum 2 + Spectrum 3
Mess of excitation spectrum (mg per inch^2)	NA	Excitation source 1: 0.72 mg	Excitation source 2: 0.11 mg	Excitation source 1: 0.72 mg Excitation source 2: 0.11mg	Excitation source 1: 0.72 mg Excitation source 2: 0.12 mg	Excitation source 1: 0.72 mg Excitation source 2: 0.13 mg
System parameters	Cross-talk loss Resonance loss SP1 (λ)	$E_{\lambda1\text{-}\lambda2,system}$ SP2 (λ)	$E_{\lambda1\text{-}\lambda3,system}$ SP3 (λ)	$E_{\lambda2\text{-}\lambda3,system}$ $A_{\lambda3,system}$ (λ)		

is a clue to decouple the mixing spectrum. Moreover, the decoupling principle is applied to analyze the spectrum of configurations 4, 5, and 6. Thus, the absorption ratio can be obtained by dividing the decoupling result of the singular emitter spectrum with that of the mixing spectrum.

To complete the process of decoupling the mixing spectrum, we access the absorption ratios of configurations 4, 5, and 6. Obviously, the absorption ratios are different because the configurations have different amounts of emission source 2, and the absorption ratio depends on the amount of emission source. In this section, we consider the model of the most closed packing and introduce the assumption that the absorption ratio is proportional to the exponential equation.

All the vital parameters can be obtained after this hybrid method. Then, the algorithm "dual emitter model" is used to simulate all the spectra by changing l and absorption coefficient in the equation of the dual emitter model. Furthermore, the results can be presented as the specific values of CIE-x, CIE-y, and lumen, which can easily map the performance at all color points. In addition, in this study, to explore whether the operation power variation affects the proportion of the overall energy loss, the above experimental analysis is repeated with different operation powers.

IV. RESULTS AND DISCUSSION

A. CROSS-TALK LOSS AND RESONANT LOSS

Fig. 5 compares the measured spectrum of configurations 1(a), 1(b), and 1(c). Configuration 1(a) is a test board with only one center LED on the same substrate. Configuration 1(b) is the actual measurement of the sample without the diffusion plate and color conversion layer lighting. Configure 1(c) shows the measurement result of the diffusion plate without the color conversion layer. The luminous power of configurations 1(a), 1(b), and 1(c) is 525.28, 472.38, and 308.33 mW, respectively. Considering the results of the spectrum measurement in Fig. 4, we can convert the power of cross-talk loss (A) and power of resonant loss (B), and we can calculate cross-talk loss rate (L_{cross_talk}) and the resonant

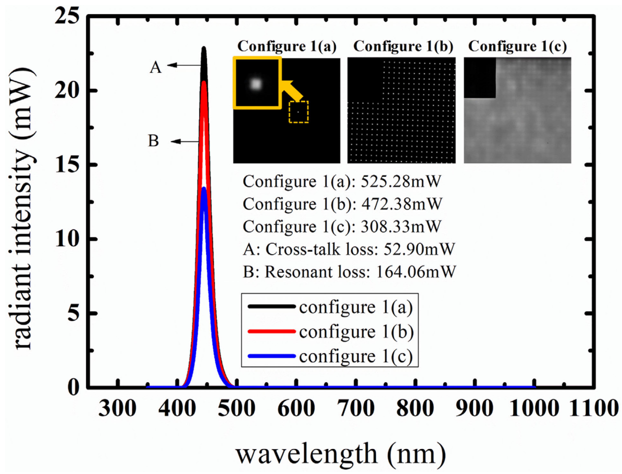

FIGURE 5. Result of cross-talk loss and resonant loss.

loss rate ($L_{resonant}$) according to the following equations:

$$A = \int_{380}^{780} \left[P1_{a(\lambda)}\right] \cdot d\lambda - \int_{380}^{780} \left[P1_{b(\lambda)}\right] d\lambda, \tag{12}$$

$$B = \int_{380}^{780} \left[P1_{b(\lambda)}\right] \cdot d\lambda - \int_{380}^{780} \left[P1_{c(\lambda)}\right] d\lambda, \tag{13}$$

$$L_{cross\_talk} = \frac{A}{\int_{380}^{780} \left[P1_{a(\lambda)}\right] * d\lambda \times 100\%}, \tag{14}$$

$$L_{resonant} = \frac{B}{\int_{380}^{780} \left[P1_{b(\lambda)}\right] * d\lambda \times 100\%}, \tag{15}$$

where $P1_{a(\lambda)}$, $P1_{b(\lambda)}$, and $P1_{c(\lambda)}$ are the measured spectra of configurations 1 (a), (b), and (c), respectively.

Fig. 5 shows the calculation by equations (12) and (13) to obtain the parameters under the following architecture: A = 52.9 mW, B = 164.06 mW, L_{cross_talk} = 10.1%, and $L_{resonant}$ = 31.2%.

B. SPECTRUM DECOUPLING

Fig. 6(a) and (b) shows the spectrum of configuration 1(c), which is called *pumping source*. The radiant flux is approximately 308.32 mW, and the full width at half maximum is approximately 18.2 nm. The parameters of the pumping source were obtained. We found that the spectrum nearly has a Gaussian distribution, which is applied to the steps in spectrum fitting.

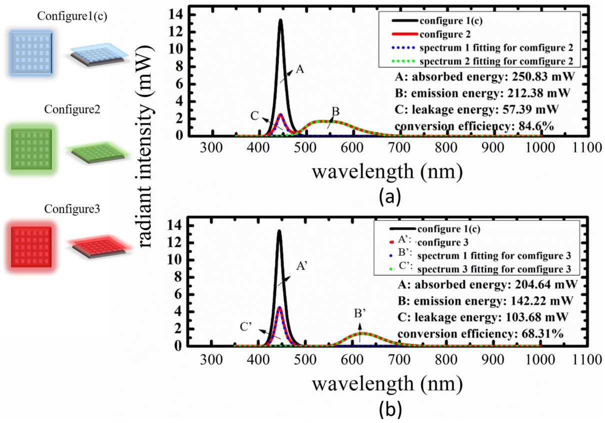

FIGURE 6. **Spectra analysis of singular-excitation spectrum and the quantum efficiency calculation result.**

Fig. 6(a) shows the spectrum of configuration 2. This configuration was prepared using the material of InGaN LED, which has the same specification as the pumping source, and the emission material with a shorter emission wavelength over other emission sources. Fig. 6(b) presents the spectrum of configuration 3. Furthermore, the emission source for configuration 3 has a longer wavelength emission spectrum, which is composed of the same materials as those for configuration 2. Both spectra can be decoupled as two parts. The first part is the Gaussian-distribution-like spectrum. It has less energy than the original energy of the pumping source because some of the energy is absorbed by the emission source for conversion into the emission spectrum. The other part is the emission spectrum, which is emitted by the energy pumping source. To obtain the key parameters for the dual phosphor modeling, we have to demarcate the spectrum needs as follows: (1) absorption energy, (2) leakage energy, and (3) emission energy.

Absorption energy is the energy absorbed by the emission source. The value of absorbed energy for emission sources 1 and 2 is the difference between the original energy of configuration 1 and the energy of the Gaussian-distribution-like spectrum decoupled from configurations 2 and 3, respectively.

Leakage energy is the energy of the pumping source absorbed by the emitter. In Figs. 6(a) and (b), the decoupled spectrum, "spectrum 1 fitting for configuration 2" in Fig. 6(a) and "spectrum 1 fitting for configuration 3" in Fig. 6(b), stand for the leakage spectrum. The energy of the leakage spectrum in Fig. 6(a) and (b) is the leakage energy. The emission energy is generated by the process of absorption and conversion of the emission source. The conversion process is described in the following equation:

$$\begin{aligned}\left[\text{Emission energy}\right] &= \left[\text{Absorbedenergy}\right]\\ &\quad\cdot\left[\text{Conversion efficiency of emission source}\right] \qquad (16)\end{aligned}$$

Therefore, the conversion efficiency of the emission source is easy to obtain, as the emission energy and absorbed energy are calculated. In this case, as shown in Fig. 6(a), the absorbed, leakage, and emission energies of the emission source 1 are 250.83, 212.38, and 57.49 mW, respectively. Similarly, the absorption, leakage, and emission energies of emission source 2 are 204.64, 142.22, and 103.68 mW, respectively. The values of the conversion efficiency ($E_{\lambda1-\lambda2,\text{system}}$ and $E_{\lambda1-\lambda3,\text{system}}$) are 84.6% and 68.31% for emitters 1 and 2, which are calculated from Fig. 6(a) and (b), respectively. SP1(λ), SP2(λ), and SP3(λ) can be expressed as follows:

$$\mathrm{SP1}\left(\lambda\right) = \frac{\mathrm{P1\_c}(\lambda)}{(\mathrm{A}+\mathrm{C})}, \qquad (17)$$

$$\mathrm{SP2}\left(\lambda\right) = \frac{\mathrm{P2\_b}\left(\lambda\right)}{B}, \qquad (18)$$

$$\mathrm{SP3}\left(\lambda\right) = \frac{\mathrm{P3}_{\mathrm{-b}(\lambda)}}{B'}, \qquad (19)$$

where P1_c(λ) is the spectrum of configuration 1(c), P2_b(λ) is *"spectrum 2 fitting for configuration 2"* in configuration 2, and P3_b(λ) is *"spectrum 2 fitting for configuration 2"* in configuration 3.

All parameters of the energy transfer from the pumping source to the emission source are obtained from the treatment of configurations 1, 2, and 3. Then, the parameters of the energy transfer from emission source 1 to emission source 2 are the most critical parameters needed, including $E_{\lambda2-\lambda3,\text{system}}$ and A(λ). To determine the absorption of the emission source 2, A(λ), the following two steps are necessary: (1) decoupling based on the principle that the photons have a longer wavelength that is not absorbed and (2) calculation of the absorption curve by dividing the decoupled spectrum and the spectrum of configuration 2, which is composed of the pumping source and the only emission source.

For configurations 4, 5, and 6, the spectrum with two emitters can be expressed as

$$\begin{aligned}\mathrm{Spectrum}\left(\lambda\right) = (\alpha SP1\left(\lambda\right) + \beta \mathrm{SP2}\ \left(\lambda\right) - \mathrm{A}\left(\lambda\right))\\ + \gamma \mathrm{SP3}\left(\lambda\right), \qquad (20)\end{aligned}$$

where α, β, and γ are the radiation power of SP1(λ), SP2(λ), and SP3(λ), respectively. αSP1(λ) + βSP2(λ) is the composition of configuration 2, and αSP1(λ) + βSP2(λ) − A(λ) can be regarded as the spectrum of configuration 2 absorbed by emitter 3. Thus, the first step is not affected by the long-wavelength part affected by the absorption spectrum is decoupling first. The decoupling process is shown in Fig. 7 (a). First, based on SP3 (λ) as the base, the long wave band of 650–700 nm is configured using configurations 4, 5, and 6. The combined result is "long wavelength fitting for configuration 4," "long wavelength fitting for configure 5," and

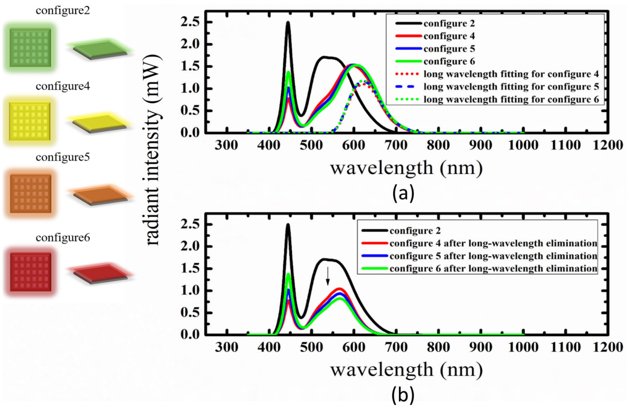

FIGURE 7. Spectra analysis of multi-excitation spectrum and the process of long-wavelength elimination.

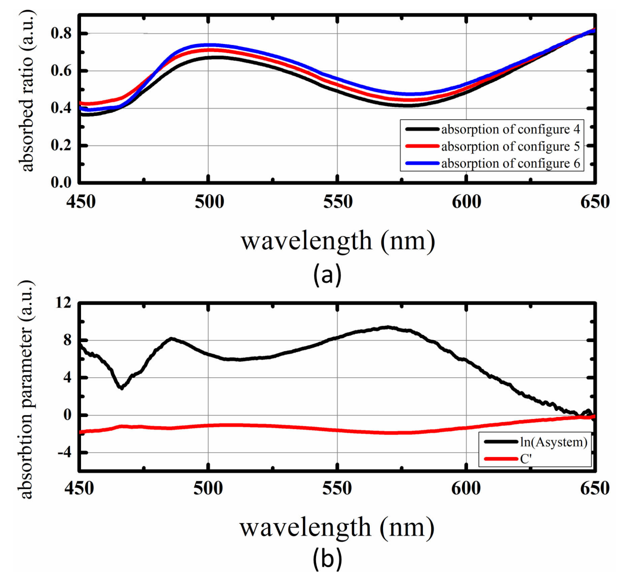

FIGURE 8. Analysis of absorption curve from long-wavelength-eliminated spectrum of configuration 4, 5, and 6.

"long wavelength fitting for configure 6." According to the fitting result, the radiated power γ of configurations 4, 5, and 6 can be obtained, as shown in Table 2.

After the long wavelength fitting is deducted, the spectrum of configurations 4, 5, and 6 is shown in Fig. 7(b). Although the combination of pumping source and emitter 2 is the same as that for configuration 2, the spectrum is affected by the unequal absorption of emitter 3. The decoupling of the short wavelength and emitter 2 occur as a result of inconsistent spectral types. Through Gaussian spectrum fitting, the SP1(λ) and SP2(λ) absorbed by emitter 3 can be calculated, and $E_{\lambda 2-\lambda 3,system}$ is calculated accordingly.

Calculation results such as table 2, $E_{\lambda 2-\lambda 3}$, system is about 73.5%.

C. RESULT OF ABSORPTION CURVE

The absorption energy at each wavelength is obtained by the method where the spectrum of configuration 2 reduces the decoupling spectrum of configurations 4, 5, and 6.

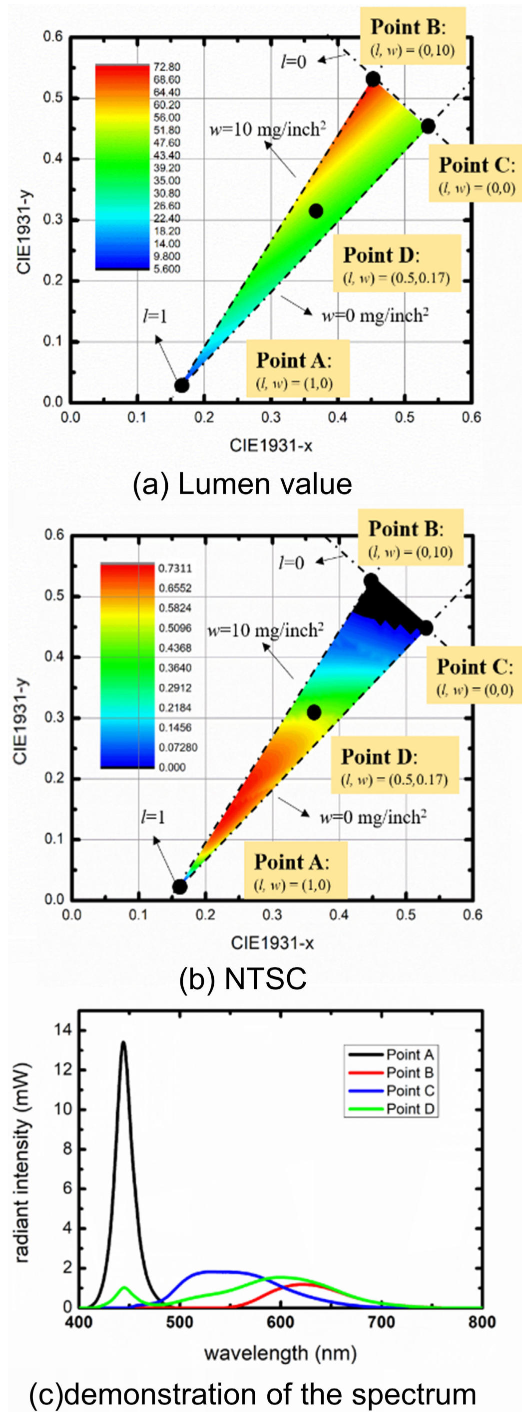

FIGURE 9. Inference (a) Lumen value (b) NTSC (c) demonstration of the spectrum, these results indicate all possible solution with the control parameter l = 0–1 and w = 0–10.

Furthermore, Fig. 8(a) shows the absorption curve obtained by dividing the absorption energy with the spectrum of configuration 2. Fig. 8(a) also shows three different absorption curves mainly because the amount of the emission source 2 has a different quantity of absorption energy.

The curves in Fig. 8(a) indicate that the characteristic of the absorption ratio differs with the wavelength. It relates

TABLE 2. Numerical analysis of multi-down-conversion efficiency.

Configuration analysis	Configuration 2	Configuration 4	Configuration 5	Configuration 6
Total power (mW)	269.88	223.28	226.40	230.07
Energy of SP3 (λ), γ (mW)		102.74	109.12	109.99
Absorbed SP1 (λ), (mW)		38.70	39.55	37.20
Absorbed SP2 (λ), (mW)		103.87	111.91	115.06
Energy of SP3 (λ) from SP1 (λ), (mW)		26.44	27.01	25.41
Energy of SP3 (λ) from SP2 (λ), (mW)		76.30	82.10	84.58
Efficiency of SP2(λ) to SP3(λ), $E_{\lambda 2\text{-}\lambda 3,system}$		73.5%	73.4%	73.5%

TABLE 3. Numerical analysis of multi-down-conversion efficiency for various operating powers.

Operating power (W)	Resonant loss	Cross-talk loss	Quantum loss 1 ($1-E_{\lambda 1\text{-}\lambda 2,system}$)	Quantum loss 2 ($1-E_{\lambda 1\text{-}\lambda 3,system}$)	Quantum loss 3 ($1-E_{\lambda 2\text{-}\lambda 3,system}$)
1	31.2%	10.1%	15.4%	31.7%	26.5%
1.5	31.4%	10.5%	15.1%	31.6%	26.4%
2	31.1%	10.3%	15.3%	31.8%	26.6%
2.5	31.8%	10.2%	15.5%	31.7%	26.6%
3	31.5%	9.9%	15.4%	31.8%	26.5%

with the characteristic of the material of emission source 2. To quantize the absorption of emission source 2, we present the hypothesis of the absorption model as a schematic in Fig. 8(a). The energy absorbed a fixed ratio as the absorb curve by the emission source 2 because the rays pass through this emission source. In the assumption of the absorption model, the total absorption ratio, At, can be written as

$$[\text{total absorbed ratio}] = \text{At} = A_{system}\left[1 - n(1 - A)\right], \quad (21)$$

where absorption A represents the absorption ratio for every particle of the emission source, and the weight index, symbol n, stands for the effective time of absorption. In addition to the above parameters, the absorption curve is also affected by the device system. The fixing intern A_{system} is added to equation (21). To analyze the parameters of the absorption curves, equation (21) can be written as follows:

$$ln\,(1 - At) = n \cdot ln\,(1{-}A) + \ln\left(A_{system}\right) \quad (22)$$

In equation (22), an important parameter is n, which is related to the weight index w for fitting with the absorption curve.

To clarify the issue of the weight index, the assumption of the excitation model is presented as equation (23). The excitation times of the emission source n is affected by optic length (OL) and the pumping probability. OL is the factor determined by the package system. Then, the pumping probability is related to the sum of the volume of the emission source (v) and the system volume (V). Then, considering the mechanism of the excitation of the emission source, we find that the excitation is proportional to the surface area of the emission source, and the fixing item $4\pi r^2/(4/3\pi r^3)$ is added to equation (23).

$$\text{n} = \text{OL}\left(\frac{\nu}{V}\right)\left(\frac{4\pi r^2}{\frac{4}{3}\pi r^3}\right) \quad (23)$$

where the effective radius of the emission source r is equal to $(3\nu/4\text{N}\pi)^{1/3}$, and the parameter N is the quantity of phosphor particles. Then, equation (23) can be arranged as follows:

$$\text{n} = \text{OL}\left(\frac{\nu}{V}\right)\left(\frac{3}{r}\right), \quad (24)$$

$$\text{n} = \text{C}w^{2/3} \quad (25)$$

where $\text{C} = \text{OL}\cdot 3^{2/3}\cdot(4\text{N}\pi)\ (1/3)/\text{Vd}^{2/3}$, d represents the density of emission source, and w represents the weight of the emission source. Then, based on the above derivation, equation (22) can be rewritten as

$$ln(1{-}\text{At}) = Cw^{2/3} ln(1 - A) + ln(A_{system}). \quad (26)$$

Thus, the mathematical equation for absorption At and the amount of emission source w can be observed. To simplify the equation, we combine the parameters of C and $(1 - \text{A})$ as C'. The equation can be rearranged as follows:

$$\ln\,(1 - \text{At}) = \text{C}'w^{2/3} + ln\left(A_{system}\right) \quad (27)$$

$$At = 1 - \exp\left[C'w^{2/3} + ln(A_{system})\right] \quad (28)$$

D. PERFORMANCE PREDICTION

After completing the above decoupling and fitting projects, we can obtain the complete module parameters and independent performance of each material in the mini-LED system, as shown in Table 3. From the results of Table 3, the different operating powers do not significantly affect the difference in the energy loss of the mini-LED module. The light conversion efficiency is mainly considered when measuring the value of P_{B-LED}. Except for this factor, all conversions and losses between light energy are not affected by the operating powers.

According to Table 3 and spectrum simulation, we can perform performance modeling of this module, as shown in Fig. 9, through the spectrum composition formula in section 2. The potential performance of the module of this material combination can be calculated, and the performance of CIE-x and CIE-y on color saturation (NTSC) and brightness (lm) can be predicted.

V. CONCLUSION

This measurement system introduces the principle of DCLE as the main principle of the decoupled spectrum and combines it with theoretical and experimental measurements, which can effectively overcome the distortion caused by the difference between the traditional simulation and material parameter measurements and the sample itself. Thus, we can measure the energy conversion loss and material parameters of the mini-LED array and predict the potential performance of this mini-LED combination.

REFERENCES

[1] W. Chen, S. N. Li, and S. Y. R. Hui, "A comparative study on the circuit topologies for offline passive light-emitting diode (LED) drivers with long lifetime & high efficiency," in *Proc. IEEE Energy Convers. Congr. Exposit.*, Sep. 2010, pp. 724–730.

[2] T. Taguchi, "Present status of energy saving technologies and future prospect in white LED lighting," *IEEJ Trans. Electr. Electron. Eng.*, vol. 3, no. 1, pp. 21–26, Jan. 2008.

[3] T. Wu, C.-W. Sher, Y. Lin, C.-F. Lee, S. Liang, Y. Lu, S.-W. H. Chen, W. Guo, H.-C. Kuo, and Z. Chen, "Mini-LED and micro-LED: Promising candidates for the next generation display technology," *Appl. Sci.*, vol. 8, no. 9, p. 1557, Sep. 2018.

[4] G. Tan, Y. Huang, M.-C. Li, S.-L. Lee, and S.-T. Wu, "High dynamic range liquid crystal displays with a mini-LED backlight," *Opt. Express*, vol. 26, no. 13, p. 16572, Jun. 2018.

[5] Z. J. Liu, W. C. Chong, K. M. Wong, K. H. Tam, and K. M. Lau, "A novel BLU-free full-color LED projector using LED on silicon micro-displays," *IEEE Photon. Technol. Lett.*, vol. 25, no. 23, pp. 2267–2270, Dec. 1, 2013.

[6] Y. Huang, G. Tan, F. Gou, M.-C. Li, S.-L. Lee, and S.-T. Wu, "Prospects and challenges of mini-LED and micro-LED displays," *J. Soc. Inf. Display*, vol. 27, no. 7, pp. 387–401, Jul. 2019.

[7] C.-H. Huang, C.-Y. Kang, S.-H. Chang, C.-H. Lin, C.-Y. Lin, T. Wu, C.-W. Sher, C.-C. Lin, P.-T. Lee, and H.-C. Kuo, "Ultra-high light extraction efficiency and ultra-thin mini-LED solution by freeform surface chip scale package array," *Crystals*, vol. 9, no. 4, p. 202, Apr. 2019.

[8] X. Bai, H. Yang, B. Zhao, X. Zhang, X. Li, B. Xu, F. Wei, Z. Liu, K. Wang, and X. W. Sun, "4-4: Flexible quantum dot color converter film for micro-LED applications," in *SID Symp. Dig. Tech. Papers, Wiley Online Library*, 2019, pp. 30–33.

[9] F. Gou, E.-L. Hsiang, G. Tan, Y.-F. Lan, C.-Y. Tsai, and S.-T. Wu, "Tripling the optical efficiency of color-converted micro-LED displays with funnel-tube array," *Crystals*, vol. 9, no. 1, p. 39, Jan. 2019.

[10] F. Gou, E.-L. Hsiang, G. Tan, P.-T. Chou, Y.-L. Li, Y.-F. Lan, and S.-T. Wu, "Angular color shift of micro-LED displays," *Opt. Express*, vol. 27, no. 12, pp. A746–A757, Jun. 2019.

[11] P. Schlotter, R. Schmidt, and J. Schneider, "Luminescence conversion of blue light emitting diodes," *Appl. Phys. A, Mater. Sci. Process.*, vol. 64, no. 4, pp. 417–418, Apr. 1997.

[12] J. Gourlay and I. Miller, "74.2: High efficiency hybrid LED backlight for large-area LCD TV," in *SID Symp. Dig. Tech. Papers, Wiley Online Library*, 2010, pp. 1097–1099.

[13] Y. Haibo, W. Zhengming, and D. Shaowu, "Performance of hydrogen maser and its usage in local atomic time at NTSC," in *Proc. IEEE Int. Freq. Control Symp. Joint 21st Eur. Freq. Time Forum*, May 2007, pp. 889–892.

[14] T.-X. Lee, K.-F. Gao, W.-T. Chien, and C.-C. Sun, "Light extraction analysis of GaN-based light-emitting diodes with surface texture and/or patterned substrate," *Opt. Express*, vol. 15, no. 11, p. 6670, 2007.

[15] D.-S. Han, J.-Y. Kim, S.-I. Na, S.-H. Kim, K.-D. Lee, B. Kim, and S.-J. Park, "Improvement of light extraction efficiency of flip-chip light-emitting diode by texturing the bottom side surface of sapphire substrate," *IEEE Photon. Technol. Lett.*, vol. 18, no. 13, pp. 1406–1408, Jul. 2006.

[16] J.-W. Pan, P.-J. Tsai, K.-D. Chang, and Y.-Y. Chang, "Light extraction efficiency analysis of GaN-based light-emitting diodes with nanopatterned sapphire substrates," *Appl. Opt.*, vol. 52, no. 7, p. 1358, Mar. 2013.

[17] M. R. Krames, O. B. Shchekin, R. Mueller-Mach, G. O. Mueller, L. Zhou, G. Harbers, and M. G. Craford, "Status and future of high-power light-emitting diodes for solid-state lighting," *J. Display Technol.*, vol. 3, no. 2, pp. 160–175, Jun. 2007.

[18] C.-H. Lin, C.-H. Huang, Y.-M. Pai, C.-F. Lee, C.-C. Lin, C.-W. Sun, C.-H. Chen, C.-W. Sher, and H.-C. Kuo, "Novel method for estimating phosphor conversion efficiency of light-emitting diodes," *Crystals*, vol. 8, no. 12, p. 442, Nov. 2018.

[19] K. Koshino, "Down-conversion of a single photon with unit efficiency," *Phys. Rev. A, Gen. Phys.*, vol. 79, no. 1, Jan. 2009.

CHE-HSUAN HUANG received the Ph.D. degree from National Chiao Tung University, Hsinchu City, Taiwan, in 2019. He is currently a Postdoctoral Fellow with the College of Materials Science and Engineering, Shenzhen University. His main research interests include advanced display and novel design methodology with rule-based and data-driven algorithm.

SHU HSIU CHANG received the B.S. degree in power mechanical engineering from National Tsing Hua University, in 2010, and the M.S. degree from the College of Photonics, National Chiao Tun University, Hsinchu City, Taiwan, where he is currently pursuing the Ph.D. degree in photonic system.

BEEN-YU LIAW received the M.S. and Ph.D. degrees from the Department of ECE, University of Missouri-Columbia, USA, in 1991 and 1995, respectively. Since 2009, he has been working on LED field, focus on package and Application integrations. He is currently with the College of Information Science and Engineering, Fujian University of Technology.

CHENG-YI LIU was born in Hualien, Taiwan. He received the Ph.D. degree in materials science and engineering from the University of California, Los Angeles, USA, in 2000.

He is currently a Professor with the Department of Chemical and Materials Engineering and the Director of the Optical Sciences Center, National Central University, Taoyuan City, Taiwan. His research interests include optoelectronic, microelectro-mechanical systems, multilayer metallization process in semiconductor, and metal nanowire.

CHIA-YUEH CHOU was born in Kaohsiung, Taiwan, in 1995. She received the B.S. degree in chemical and materials engineering from Tunghai University, Taichung City, Taiwan, in 2017. She is currently pursuing the Ph.D. degree in chemical and materials engineering with National Central University, Taoyuan City, Taiwan.

Her research interests include optoelectronic systems, ceramic materials, transparent conductive layer, and thin-film capacitor used in semiconductor.

JIA-ROU ZHOU received the B.S. degree from the Department of Physics, Chung Yuan University, Taoyuan City, Taiwan, in 2018. She is currently pursuing the M.S. degree with the Institute of EO Engineering, National Chiao Tung University, Hsinchu City, Taiwan.

CHIEN-CHUNG LIN (Senior Member, IEEE) received the B.S. degree in electrical engineering from National Taiwan University, in 1993, and the M.S. and Ph.D. degrees in electrical engineering from Stanford University, Stanford, CA, USA, in 1997 and 2002, respectively. His thesis work focused on design, modeling, and fabrication of micromachined-tunable optoelectronic devices. Since 2009, he has been with National Chiao Tung University (NCTU), Tainan, Taiwan, where he holds a position as a Professor. The major research efforts in his group are in design and fabrication of novel semiconductor optoelectronic devices, including LEDs, solar cells, and lasers, since 2016.

HAO-CHUNG KUO (Fellow, IEEE) received the B.S. degree in physics from National Taiwan University, Taipei, Taiwan, the M.S. degree in electrical and computer engineering from Rutgers University, New Brunswick, NJ, USA, in 1995, and the Ph.D. degree from the University of Illinois at Urbana–Champaign, Champaign, IL, USA, in 1999. He is currently the Associate Dean of the Office of International Affair, National Taiwan University.

LI-JUN SONG is currently working for power electric design in Winsemi. He is following the research of GaN power device and controller.

FENG LI received the bachelor's degree in communication engineering from Sanxia University, in 2019. He is currently pursuing the master's degree with the College of Materials Science and Engineering, Shenzhen University. His main research interests include new semiconductor device structure and GaN diodes.

XINKE LIU (Member, IEEE) received the B.Appl.Sc. degree (Hons.) in materials science and the Ph.D. degree in electrical and computer engineering from the National University of Singapore, in 2008 and 2013, respectively. He is currently an Assistant Professor/Research Professor with Shenzhen University, China. He has authored or coauthored more than 100 journal and conference papers, and his research is related to novel material and devices.